Bakker, T.; Asselt, C.J. van; Bontsema J.; Müller, J.; Straten, G. van, 2007. Path following with a robotic platform. In: Agricontrol 2007. 2nd IFAC International Conference on Modeling and Design of Control Systems in Agriculture. Osijek, Croatia. pp. 153-158.

PATH FOLLOWING WITH A ROBOTIC PLATFORM

Tijmen Bakker [*] **Kees van Asselt** [*] **Jan Bontsema** [**]
Joachim Müller [***] **Gerrit van Straten** [*]

[*] *Wageningen University, Systems and Control Group,*
P.O. Box 17, 6700 AA Wageningen, The Netherlands
email: tijmen.bakker@wur.nl
[**] *Wageningen UR Horticulture, P.O. Box 17, 6700 AA*
Wageningen, The Netherlands
[***] *University of Hohenheim, Institute for Agricultural*
Engineering, 70593 Stuttgart, Germany

Abstract: This paper considers path following control for a four-wheel steered robotic platform. The vehicle used for the experiments is a specially designed robotic platform for performing autonomous weed control. The robot uses RTK-DGPS to determine both position and orientation relative to the path. The deviation of the robot to the desired path is supplied to a high level controller that determines the setpoints of the wheel angles and wheel speeds. At low level each wheel angle is controlled by a P controller combined with a Smith predictor. Results are presented of a preliminary navigation test on a paving. *Copyright © 2007 IFAC*

Keywords: Autonomous mobile robots, Autonomous vehicles, Four-wheel drive, Four-wheel steering, Global positioning systems, Robot navigation, Robot control, Robots

1. INTRODUCTION

In organic farming there is a need for weeding robots that can replace manual weeding. The required labour for hand weeding is expensive and often difficult to obtain. In 1998 in the Netherlands on average 73 hours hand weeding were spend on one hectare of sugar beet (Weide, *et al.*, 2002). In this paper a path following control system for a weeding robot is presented enabling the robot to navigate autonomously along a path.

A common design for a control system for agricultural vehicles is to split up the control system in a low level and a high level controller (Bendtsen, *et al.*, 2002; Bak and Jakobsen, 2004). The low level electro-hydraulic system is a system with dead time. A well known method to compensate for time delays is the Smith predictor. Ge and Ayers (1991) applied this successfully to control an electro-hydraulic system on a hydraulic test bench. We used a Smith Predictor to compensate for time delays in the application of an electro-hydraulic steering system in practice.

The high level system is partly inspired by work of Hague and Tillett (1996) and Bendtsen, *et al.* (2002). Bendtsen, *et al.* (2002) uses a model for a four-wheel steered vehicle derived from Campion, *et al.* (1996) and presents simulation studies ap-

Fig. 1. Robot platform

plying feedback linearization as a control method. Hague and Tillett (1996) worked out a method for path following with a more straightforward approach, but this is applied for a vehicle with two driven wheels and two free rolling wheels.

2. ROBOTIC PLATFORM

2.1 Platform

The vehicle used for the experiments is a specially designed robotic platform for performing autonomous weed control (figure 1). The design of the platform was described earlier by Bakker, *et al.* (2006). The platform is four-wheel steered and four-wheel driven. There is no mechanical constraint on the maximum turning angle of a wheel around its vertical axis. Power is provided by a diesel engine that powers the wheels via an hydraulic transmission. The hydraulic transmission consists of a pump supplying oil to eight proportional valves, each connected to one fixed displacement hydraulic motor. Four hydraulic motors are used to drive the wheels, the other four to steer the wheels. Computer control of the valves is achieved using pulse width modulation via two micro-controllers connected to a CAN bus. The pump/valves combination is a 'load sensing' system: the pressure drop over the valves controls the displacement of the pump via an hydraulic load sensing connection and is limited to a small value, independent of load pressure.

2.2 Electronics

The weeding robot electronics consists of 7 embedded controllers connected by a CAN bus using the ISO 11783 protocol. In the inside of every wheel rim a cogwheel is mounted for wheel speed measurement. The two magneto resistive sensors per cogwheel are placed in such a way that the direction of rotation can be resolved. The rotation

of the wheels is measured by these sensors with a resolution of 100 pulses per wheel revolution. The wheel angle of each wheel is measured by a Kverneland 180 degree sensor with an accuracy of one degree. Per wheel a micro controller is mounted transmitting wheel speed and wheel angles via the CAN bus. Two GPS antennas are used to measure both vehicle position and orientation. Both are connected to a Septentrio PolaRx2eH RTK-DGPS receiver with a specified position accuracy of 1-2 cm and a specified orientation accuracy of 0.3 degrees (1σ, with σ the standard deviation of the error). The two GPS antennas are mounted on a metal plate to prevent multipath errors. A base station with a Septentrio PolaRx2e RTK-DGPS supplies the RTK-correction signals via a radio connection to the Septentrio PolaRx2eH receiver. The position of the base station itself is configured by a correction supplied by the service of a company called 06-GPS via GPRS. One embedded controller running a real time operating system (National Instruments PXI system) also connected to the CAN bus does the vehicle control. The GPS receiver, and a radio modem are connected to the PXI via RS232. The radio modem interfaces the remote control used for manual control of the weeding robot. The manual control is used for guaranteeing safety during field trials and for transportation to and from the field. The PXI system gathers wheel angles, wheel speeds, crop row location data, GPS data and remote control data and controls the vehicle by sending messages to the two micro controllers connected to the hydraulic valves.

3. PATH FOLLOWING STRUCTURE

The vehicle control consists of two levels. At high level the wheel angle setpoints and wheel speed setpoints are determined in order to decrease the deviation from the path and the error in orientation. At low level, controllers are used to realize the wheel angles and wheel speeds determined by the high level control.

The deviation and the orientation error of the robot from a path are determined by a specially designed orthogonal projection on the path using the measured orientation and the GPS position. The orthogonal projection is designed to calculate the deviation and the orientation error relative to a line of positions $y(x)$.

4. LOW LEVEL CONTROL

4.1 Wheel angle process model

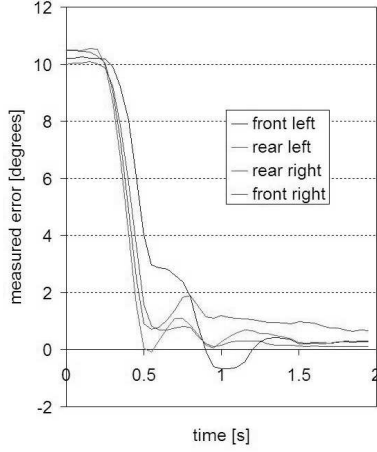At low level for each wheel the wheel angle and wheel speed are controlled. The hydraulic valves

Fig. 2. Performance of the wheel angle control, average of 96 measurements. The setpoint changes at t=0 from 10 to 0 degrees.

used for steering the wheels of the weeding robot have a certain reaction time, resulting in a time delay of the steering. Furthermore, if a valve has an open time of less than a dead time, a control does not have any effect. So the wheel angle process can be represented by:

$$\dot{\beta} = 0 \qquad \qquad for \ t_{open} \ < t_{dead} \quad (1)$$

$$\dot{\beta} = K_p \cdot u(t - t_d) \qquad for \ t_{open} \ > \ t_{dead} \quad (2)$$

and:

$$u(t) = -1995 \qquad if \ U < 2500$$
$$u(t) = U - 4495 \qquad if \ 2500 \le U \le 4000$$
$$u(t) = 0 \qquad if \ 4000 < U < 6000$$
$$u(t) = U - 5405 \qquad if \ 6000 \le U \le 7500$$
$$u(t) = 2095 \qquad if \ U > 7500$$

where:

$\dot{\beta}$ is the wheel steering angle speed [$°/s$].

K_p is the gain of the process and equals 0.0712.

u is the control corrected for the dead band.

U is the control [$\%U_{DC} \cdot 100$].

U_{DC} is the power supply voltage and equals about 12 [V].

t_d is the delay of the system and equals 0.25 [s].

t_{open} is the total time where $U < 4000$ or the total time where $U > 6000$.

t_{dead} is the dead zone of the system and equals 0.15 [s].

K_p is determined from step responses of the system.

4.2 Wheel angle control

To compensate for the time delay a P controller with Smith predictor is used for the wheel steering control (Stephanopoulos, 1984).
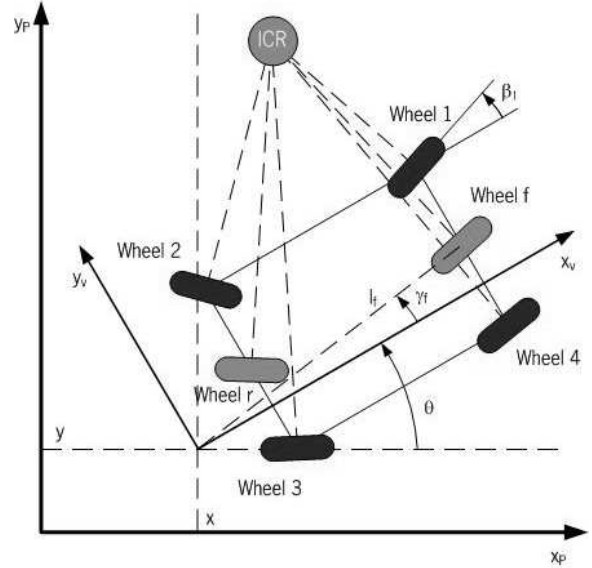

Fig. 3. Robot with ICR

The wheel angle control of the robot was tested by applying setpoint changes to one wheel while the robot was standing still on a flat concrete floor. From some first measurements it appeared that at large setpoint changes the variable pump controlled by the load sensing system could not react fast enough for the change in the flow required to maintain full pressure in the hydraulic system. Furthermore, if we imagine the robot driving over the field, the flow needed for steering will require only small changes in the flow already present for driving. So to simulate the presence of a continuous oil flow for driving during the wheel angle control test, one wheel was lifted from the floor and a constant control was put on the valve controlling its speed.

The average error of a series of 96 measurements on a wheel angle setpoint change of 10 degrees decreased within one second to zero plus or minus 2 degrees (see fig. 2).

5. HIGH LEVEL CONTROL

5.1 Vehicle model

The point of the vehicle that should follow the path is the vehicle implement attached to the vehicle. Consider a path-relative coordinate system (x_P, y_P) as illustrated in 3. The implement position is then completely described by $\xi = [x \ y \ \theta]^T$ where x denotes the distance along the path, y the perpendicular offset from the path, and θ the heading angle of the platform relative to the tangent direction of the path at the point at the foot of the perpendicular.

Consider a coordinate system (x_v, y_v) fixed to the robot frame. The position of a wheel in this vehicle coordinate system is characterized by the angle γ_i

and the distance l_i where i is the wheel index. The orientation of a wheel relative to x_v is denoted β_i. The model assumes pure rolling and non-slip conditions and driving in a horizontal plane. Therefore the motion of the robot can always be viewed as an instantaneous rotation around the instantaneous center of rotation (ICR). At each instant, the orientation of any wheel at any point of the robot frame must be orthogonal to the straight line joining its position and the ICR. The two-dimensional location of the ICR is specified by the angles of two wheels. For convenience a virtual front wheel β_f and a virtual rear wheel β_r is introduced with corresponding γ_f, l_f, γ_r and l_f, respectively located right in between the front wheels and right in between the rear wheels. The motion of the vehicle implement is described the following state-space model derived from earlier work from Campion, *et al.* (1996) and Bendtsen, *et al.* (2002):

$$\dot{\xi} = R^T(\theta)\Sigma(\beta_i)\eta \tag{3}$$

where $R(\theta)$ is the orthogonal rotation matrix:

$$R(\theta) = \begin{bmatrix} \cos(\theta) & \sin(\theta) & 0 \\ -\sin(\theta) & \cos(\theta) & 0 \\ 0 & 0 & 1 \end{bmatrix} \tag{4}$$

and:

$$\Sigma(\beta_i) = \begin{bmatrix} l_f\cos(\beta_r)\cos(\beta_f - \gamma_f).. \\ \quad - l_r\cos(\beta_f)\cos(\beta_r - \gamma_r) \\ l_f\sin(\beta_r)\cos(\beta_f - \gamma_f).. \\ \quad - l_r\sin(\beta_f)\cos(\beta_r - \gamma_r) \\ \sin(\beta_f - \beta_r) \end{bmatrix} \tag{5}$$

So here the β_i are considered as inputs.

It is assumed that the robot does not need to just turn around the implement position, where $\dot{x}$ and $\dot{y}$ are both zero while η is not zero. It follows:

$$\eta = \frac{v}{\sqrt{([R^T(\theta)\Sigma(\beta_i)]_{11})^2 + [R^T(\theta)\Sigma(\beta_i)]_{21})^2}} \tag{6}$$

The wheel orientation β_3 and β_4 follow from β_f and β_r as described by Bendtsen, *et al.* (2002) and Sørensen (2002) and β_1 and β_2 can be found in a similar way:

$$\beta_1 = \arctan\left(\frac{L\sin(\beta_f)\cos(\beta_r)}{L\cos(\beta_f)\cos(\beta_r) - \frac{1}{2}W\sin(\beta_f - \beta_r)}\right)$$

$$\beta_2 = \arctan\left(\frac{L\cos(\beta_f)\sin(\beta_r)}{L\cos(\beta_f)\cos(\beta_r) - \frac{1}{2}W\sin(\beta_f - \beta_r)}\right)$$

$$\beta_3 = \arctan\left(\frac{L\cos(\beta_f)\sin(\beta_r)}{L\cos(\beta_f)\cos(\beta_r) + \frac{1}{2}W\sin(\beta_f - \beta_r)}\right)$$

$$\beta_4 = \arctan\left(\frac{L\sin(\beta_f)\cos(\beta_r)}{L\cos(\beta_f)\cos(\beta_r) + \frac{1}{2}W\sin(\beta_f - \beta_r)}\right) \tag{7}$$

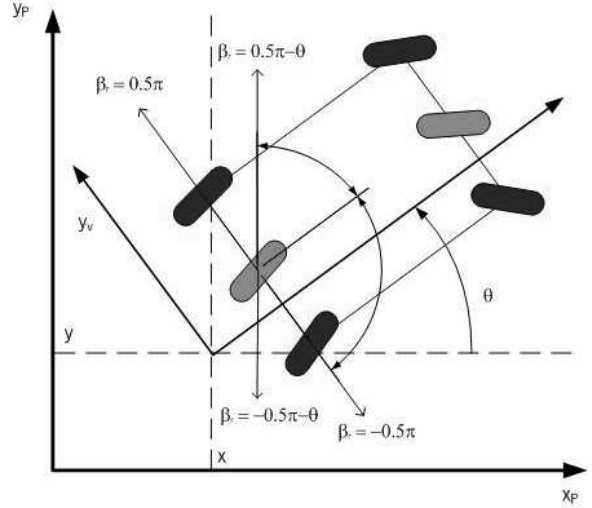Fig. 4. Robot with constraints. In this situation β_r is constrained by -0.5π and $0.5\pi - \theta$.

where L is the distance between the front and rear wheels and W the distance between the left and right wheels.

The wheel angular speeds $\dot{\phi} = [\dot{\phi}_1, \dot{\phi}_2, \dot{\phi}_3, \dot{\phi}_4]^T$ are controlled at low level, and follow from the vehicle model:

$$\dot{\phi} = J_2^{-1}J_1(\beta_i)\Sigma(\beta_i)\eta(t) \tag{8}$$

where:

$$J_1(\beta_i) = \begin{bmatrix} \cos(\beta_1) & \sin(\beta_1) & l_1\sin(\beta_1 - \gamma_1) \\ \cos(\beta_2) & \sin(\beta_2) & l_2\sin(\beta_2 - \gamma_2) \\ \cos(\beta_3) & \sin(\beta_3) & l_3\sin(\beta_3 - \gamma_3) \\ \cos(\beta_4) & \sin(\beta_4) & l_4\sin(\beta_4 - \gamma_4) \end{bmatrix}$$

$$J_2 = \begin{bmatrix} r_1 & 0 & 0 & 0 \\ 0 & r_2 & 0 & 0 \\ 0 & 0 & r_3 & 0 \\ 0 & 0 & 0 & r_4 \end{bmatrix} \tag{9}$$

and r_1, r_2, r_3, r_4 are the radii of the four wheels.

5.2 Path following controller design

Let $\dot{\theta} = d_1$ and $\dot{y} = d_2$. The path tracking controller must thus compute d_1 and d_2 (and consequently $\beta_{f,sp}$ and $\beta_{r,sp}$) in order to minimize θ and y. Since we use a path-relative coordinate system, a controller is designed which computes d_1 and d_2:

$$d_1 = K_\theta\theta \tag{10}$$

$$d_2 = K_y y \tag{11}$$

For both K_y and K_θ constant values are used chosen by simulation to give the desired response and both are equal to -1.

Consider $\beta_{r,sp}$. Although there is no mechanical constraint on the wheel angles we introduce the following constraint to prevent twisting of the cables from the wheel speed sensors:
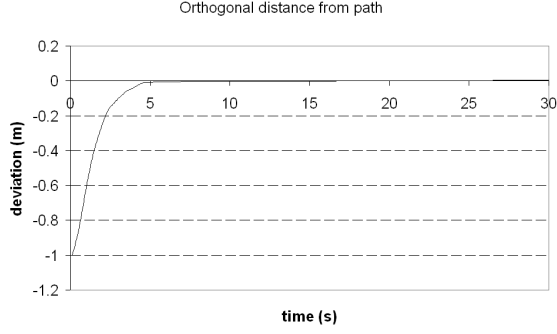
$$-0.5\pi < \beta_{r,sp} < 0.5\pi \tag{12}$$
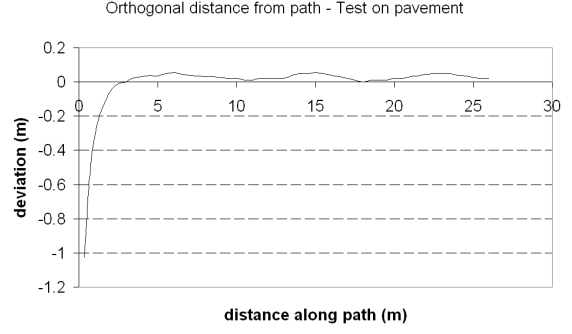
Fig. 5. Hardware in the loop performance of path following.

Fig. 6. Path following performance from a test on a pavement

5.3 Hardware in the loop simulation results

The wheels should never turn in a direction causing the wheel to drive along the path in opposite direction, so $\beta_{r,sp}$ must also fulfill the following constraints, as can be seen from figure 4

$$-0.5\pi - \theta < \beta_{r,sp} < 0.5\pi - \theta \qquad (13)$$

These constraints hold also for $\beta_{f,sp}$. Because from $R^T(\theta)\Sigma(\beta_i)$ follows:

$$\beta_{f,sp} = \beta_{r,sp} + asin(d_1) \qquad (14)$$

the following constraints hold for $\beta_{r,sp}$:

$$\begin{aligned}\beta_{r,sp,max} = \min(0.5\pi, \ 0.5\pi - \theta, .. \\ 0.5\pi - asin(d_1), .. \\ 0.5\pi - \theta - asin(d_1))\end{aligned} \quad (15)$$

$$\begin{aligned}\beta_{r,sp,min} = \max(-0.5\pi, \ 0.5\pi - \theta, .. \\ -0.5\pi - asin(d_1), .. \\ -0.5\pi - \theta - asin(d_1))\end{aligned} \quad (16)$$

$\beta_{f,sp}$ can now be found solving $\beta_{r,sp}$ from equation 3 substituting d_2 for $\dot{y}$ ($R^T(\theta)\Sigma(\beta_{r,sp})$ is a 3x1 matrix):

$$d_2(\beta_{r,sp}) = ..$$
$$\frac{[R^T(\theta)\Sigma(\beta_{r,sp})]_{21}}{\sqrt{(([R^T(\theta)\Sigma(\beta_{r,sp})]_{11})^2 + ([R^T(\theta)\Sigma(\beta_{r,sp})]_{21})^2)}} \qquad (17)$$

$\beta_{r,sp}$ is solved from this equation by calculating $d_2(\beta_{r,sp})$ for every $\beta_{r,sp}$ in the range $\beta_{r,sp,min} < \beta_{r,sp} < \beta_{r,sp,max}$. $\beta_{r,sp}$ is found for $d_2(\beta_{r,sp})$ closest to the controller output d_2. $\beta_{f,sp}$ follows from 14.

The wheel speed setpoints follow then from 8, but are constrained by the maximum wheel speed of the robot $\dot{\phi}_{max}$. Therefore $\dot{\phi}$ is finally corrected for $\dot{\phi}_{max}$:

$$\begin{aligned}\frac{\dot{\phi}_i}{max(\dot{\phi}_i)}\dot{\phi}_{max} \qquad & if \ max(\dot{\phi}_i) > \dot{\phi}_{max} \\ \dot{\phi}_i \qquad & if \ max(\dot{\phi}_i) <= \dot{\phi}_{max}\end{aligned} \quad (18)$$

The performance of the control was evaluated in a hardware-in-the-loop test. The robot was mounted on trestles and the robot dynamics of the low level control were included in a closed loop. The robot motion in the x,y-plane was calculated by 3. The robot was set at an offset of one meter from a straight path, with the same orientation as the path. The robot was then set to autonomous control and followed the line autonomously. The orthogonal offset from the line was logged at a time interval of 50 ms. Results are visualized in figure 5.

6. EXPERIMENTAL RESULTS

The performance of the control was also evaluated with the robot on a paving. A rope was tightly stretched between two pins fixed in the pavement over a distance of about 30 meters. The two ends were surveyed using the base station RTK-DGPS receiver as rover with DGPS correction from the service provided by 06-GPS. Then the RTK-DGPS was reinitialized as base station. The path consisting of the surveyed points was entered via the robot user interface. A weeding unit with a chalk holder was attached to the robot (see fig. 7) holding about 2 cm wide chalks. The robot was positioned about 1 meter from the rope, approximately in the same direction as the straight line by manual control. Then the rope was removed and the robot was set to autonomous control and followed the path autonomously. The speed of the robot was about 0.5 m/s.

The rope was then tightened again between the two pins and at regular distances of 50 cm along the rope the orthogonal distances from the rope to the middle of the chalk line was measured manually. At the start of the chalk line some more orthogonal distances were measured at 20 cm from each other. The results are visualized in figure 6. After the initial error was controlled at about 3 meters of travel, the maximum deviation was 6

Fig. 7. Chalk holder attached to the robot. To the right of the the robot the rope indicating the path is visible

cm. The average deviation over this distance was 3 cm and the standard deviation was 1.5 cm.

7. CONCLUSION

The development in this paper was based on achieving a simple and easy to implement controller. The machine in the loop procedure allows a very practical way of tuning the controller. It may seem surprising at first that a P controller can do the track following, given the fact that the steering system is highly non-linear. However, by using the inverse kinematics the system becomes linear, and since our system is a mechanical system consisting of two pure integrators, using a P controller is a natural choice.

The Smith predictor compensates well for time-delays in electro-hydraulic steering systems in practice. The high level control method presented in this paper has a good performance. Further improvements of the standard deviation are not to be expected because it is about equal to the RTK-DGPS accuracy, but the average error of 3 cm needs some more investigation.

The high level control method parameters K_y and K_θ are easy to tune and taking virtual wheels as a base for the controller eliminates the need of at least one discrete state of the hybrid approach as presented by Bak, *et al.* (2003). Also, in contrary to a feedback linearization-based approach like Bendtsen, *et al.* (2002), this approach gives the possibility to deal with limitations on the wheel-angles as they exist on almost every four-wheel steered vehicle in practice.

The path following system will be tested more extensively on other path shapes, and at least on a typical headland path. Then the path following system will be extended with a vision based row detection system. Combining both crop row fol-

lowing and path following with GPS should enable the robot to navigate autonomously over a whole field.

REFERENCES

Bak, T., J. Bendtsen and A.P. Ravn (2003). Hybrid control design for a wheeled mobile robot. In *Hybrid Systems: Computation and Control, Proceedings*, volume 2623 of *Lecture Notes in Computer Science*, pages 50–65.

Bak, T. and H. Jakobsen (2004). Agricultural robotic platform with four wheel steering for weed detection. *Biosystems Engineering*, 87(2): 125–136.

Bakker, T., C.J. Asselt, J. Bontsema, J. Müller and G. van Straten (2006). An autonmous weeding robot for organic farming. In P. Corke and S. Sukkarieh, editors, *Field and Service Robotics*, STAR, pages 579–590. Springer-Verlag Berlin Heidelberg, 25 edition.

Bendtsen, J.D., P. Andersen and S. Pedersen (2002). Robust feedback linearisation-based control design for a wheeled mobile robot. In *6th International Symposium on Advanced Vehicle Control (AVEC '02)*, Hiroshima, Japan.

Campion, G., G. Bastin and B. DandreaNovel (1996). Structural properties and classification of kinematic and dynamic models of wheeled mobile robots. *IEEE Transactions on Robotics and Automation*, 12(1):47–62.

Ge, J. and P.D. Ayers (1991). Design of controllers for nonlinear electrohydraulic systems with time delays. *Transactions of the Asae*, 34 (3):1016–1022.

Hague, T. and N.D. Tillett (1996). Navigation and control of an autonomous horticultural robot. *Mechatronics*, 6(2):165–180.

Sørensen, M.J. (2002). *Modelling and control of wheeled Farming Robot*. Msc thesis, Aalborg University.

Stephanopoulos, G., 1984. *Chemical process control. An Introduction to Theory and Practice*. Prentice/Hall International, Inc., London.

Weide, R.Y. van der, L.A.P. Lotz, P.O. Bleeker, and R.M.W. Groeneveld (2002). Het spanningsveld tussen beheren en beheersen van onkruiden op biologische bedrijven. In F.G. Wijnands, J.J. Schroder, W. Sukkel, and R. Booij, editors, *Themaboek 303. Biologisch bedrijf onder de loep*, pages 129–138. Wageningen Universiteit, Wageningen.